Synthesis and DNA interactions of a bis-phenothiazinium photosensitizer†

Beth Wilson,[a] María-José Fernández,[b] Antonio Lorente*[b] and Kathryn B. Grant*[a]

Received 17th June 2008, Accepted 29th July 2008
First published as an Advance Article on the web 9th September 2008
DOI: 10.1039/b810015b

We report the synthesis and characterization of *N*,*N*′-bis[(7-dimethylamino)phenothiazin-5-ium-3-yl]-4,4′-ethylenedipiperidine diiodide (**3**), consisting of two photosensitizing phenothiazinium rings attached to a central ethylenedipiperidine linker. At all time points (10, 30, 60 min) and all wavelengths (676, 700, 710 nm) tested, photocleavage of pUC19 plasmid DNA (22 °C and pH 7.0) was markedly enhanced by 1 μM of **3** in comparison to 1 μM of the parent phenothiazine methylene blue (**MB**). At concentrations of phenothiazine ranging from 5 to 0.5 μM, the photocleavage levels produced by compound **3** were consistently higher than the cleavage produced using approximately twice the amount of **MB** (*e.g.*, 710 nm irradiation of 5 μM of **3** and 10 μM of **MB** cleaved the plasmid DNA in 93% and 71% yields, respectively). Scavenger assays provided evidence for the involvement of singlet oxygen and, to a lesser extent, hydroxyl radicals in DNA damage. Analysis of photocleavage products at nucleotide resolution revealed that direct strand breaks and alkaline-labile lesions occurred predominantly at guanine bases. While compound **3** and **MB** were both shown to stabilize duplex DNA, the ΔT_m values of calf thymus (CT) and *C. perfringens* DNAs were approximately three fold higher in the presence of compound **3**. Finally, viscometric data indicated that CT DNA interacts with compound **3** and **MB** by a combination of groove binding and monofunctional intercalation, and with compound **3** by a third, bisintercalative binding mode.

Introduction

In photodynamic therapy (PDT), photosensitizing drugs are employed to effectively treat a variety of malignant tumors and non-cancerous diseases.[1] PDT offers the advantage of selective localization and light activation of the photosensitizer in diseased tissue, thereby minimizing damage to healthy cells. Notwithstanding, only a few drugs, mostly first and second generation porphyrin derivatives, have been approved clinically.[1b] There is now great interest in the development of alternative photosensitizing agents. An important requirement of PDT is strong absorption of light within a therapeutic window of 600–800 nm.[1b,c] These longer wavelengths reduce light scattering and are more readily transmitted by biological constituents, thereby providing maximal light penetration. At wavelengths greater than 800 nm, photons do not possess the necessary energy required by the sensitizer triplet state to excite ground state molecular oxygen.

The phenothiazine dye methylene blue (**MB**; Scheme 1) strongly absorbs light at 664 nm. With regards to PDT, **MB** has demonstrated efficient photodynamic activity in several malignant cell lines,[2] murine tumor models,[3] and in the palliation of inoperable human esophageal cancer[4a] and AIDS-related Kaposi's sarcoma.[4b] Additionally, **MB** has been employed in anti-microbial research.[5] Specifically, **MB** has exhibited photoinactivation of bacterial pathogens including *Bacillus anthracis*, the causative agent of anthrax,[5c] and methicillin-resistant, epidemic strains of *Staphylococcus aureus*.[5b] **MB** photosensitization is in current use to inactivate the human immunodeficiency virus HIV-1 in donated blood products.[5a,e] A recent study has indicated that phototreatment of cell cultures in the presence of **MB** abolishes the infectivity of West Nile virus.[5d]

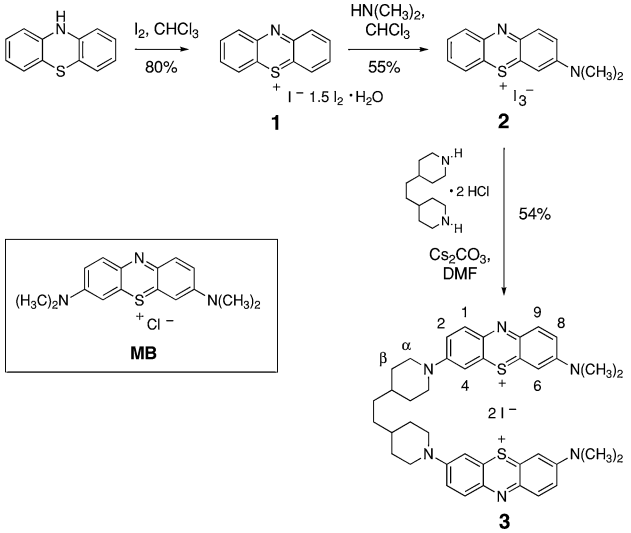

Scheme 1 Structure of methylene blue and transformation of 10*H*-phenothiazine **1** to bis-(phenothiazinium)ethylenedipiperidine salt **3**.

[a]*Department of Chemistry, Georgia State University, P.O. Box 4098, Atlanta, GA, 30302-4098, USA. E-mail: kbgrant@gsu.edu; Fax: +1-404-413-5505; Tel: +1-404-413-5522*
[b]*Departamento de Química Orgánica, Universidad de Alcalá, 28871, Alcalá de Henares (Madrid), Spain. Email: antonio.lorente@uah.es; Fax: +91 8854686; Tel: +91 8854691*

† Electronic supplementary information (ESI) available: Experimental details concerning the preparation of known compounds **1** and **2**, ^{1}H NMR, ^{13}C NMR and HMQC NMR spectra of compound **3**, viscometric plots of alternating poly[(dA-dT)]$_2$ and poly(dA)·poly(dT) pre-equilibrated with compound **3** and with **MB**, UV–visible absorbance data and spectra for compound **3** and **MB** in solutions containing 1 μM of dye in the presence and absence of CT DNA and 1% SDS. See DOI: 10.1039/b810015b

Methylene blue meets two additional important criteria of PDT: low levels of cytotoxicity in the absence of irradiation and preferential retention by diseased tissue.[1,2] As a result, **MB** has been employed as a staining agent for tumor detection *in vivo*.[6] Low toxicity levels have permitted other non-PDT clinical applications, which include the use of **MB** to identify sentinel lymph nodes in cancer staging,[7] and as an effective treatment for ifosfamide-induced encephalopathy[8a] and methemoglobinemia.[8b]

While methylene blue has been reported to accumulate in mitochondria and lysosomes,[9] Rück and co-workers have demonstrated that irradiation triggers its re-localization from lysosomes to the cell nucleus.[9a] **MB** is positively charged at physiological pH ($pK_a > 12.0$),[10] rendering DNA an attractive biological target. In fact, it has been well established that **MB** can non-covalently bind to DNA ($K_a = 7–10 \times 10^5$ M^{-1}), by exhibiting one of two different binding modes (intercalation or groove binding), as a function of DNA sequence and experimental conditions.[11] Its close association with DNA and efficient singlet oxygen production form a basis for effective oxidative photodamage by **MB**.[2,12] Although enzymatic reduction of phenothiazinium chromophores to the photoinactive, leuco form can reduce photodynamic action, methylation of methylene blue at the 1 and/or position 9 of the phenothiazinium ring has been shown to prevent and/or inhibit the reduction process and increase singlet oxygen yields.[5e,12b]

In spite of the many advantages of **MB**, the use of phenothiazine-based chromophores in PDT has remained relatively unexplored. Herein we report the synthesis and characterization of photosensitizer **3** in which two phenothiazine intercalating units are attached covalently by a semi-rigid, electron donating ethylenedipiperidine linker. (In a previous study, the substitution of ethylenedipiperidine into the linking chain of ditercalinium was shown to promote stronger bisintercalation into double-helical DNA with appropriate placement of the linker in the major groove of the helix.[13]) Our goal was to design a reagent capable of photocleaving DNA more efficiently and at longer wavelengths than **MB**.

Results and discussion

Synthesis

Bis-(phenothiazinium)ethylenedipiperidine salt **3** was synthesized according to the procedures depicted in Scheme 1. The precursors **1** and **2** are known compounds[14] and were prepared following a commonly utilized route for the synthesis of 3-(dialkylamino)phenothiazin-5-ium salts with the exception of changing the solvent from methanol to chloroform in the preparation of compound **2**. While syntheses of other 3,7-disubstituted phenothiazin-5-ium salts have been reported,[14,15] the nucleophilic attachment of an ethylenedipiperidine linker chain to two equivalents of **2** to form dicationic **3** required the exploration of a number of different solvents (*e.g.*, methanol, chloroform, DMSO) and counterions (*e.g.*, hexafluorophosphate). The synthesis of the iodide salt of **3** was finally achieved in DMF using caesium carbonate as base. Purification of the reaction products by silica gel flash column chromatography and subsequent recrystallization from methanol yielded pure compound **3** as a dark-blue solid in 54% yield.

Table 1 Electronic absorption data[a]

Compound	λ_{max}/nm	$\varepsilon \times 10^4/M^{-1}$ cm^{-1}	$\varepsilon \times 10^4/M^{-1}$ (bp) cm^{-1}
3	615	*nd*	*na*
3 + 1% SDS	675	14.5	*na*
3 + DNA	680	*na*	7.78
MB	664	6.43	*na*
MB + 1% SDS	661	7.84	*na*
MB + DNA	675	*na*	5.80

[a] Extinction coefficients for compound **3** and **MB** were determined in 10 mM sodium phosphate buffer pH 7.0 using solutions containing 1 to 10 μM of dye in the presence and absence of 1% SDS (w/v) or 38 to 380 μM bp CT DNA. The λ_{max} values were obtained from the spectra recorded at 10 μM concentrations of phenothiazine. The samples containing DNA were pre-equilibrated for 12 h in the dark at 22 °C. *na* = not applicable; *nd* = not determined due to aggregation in buffer.

UV–visible spectrophotometry

In our first set of experiments, we recorded UV–visible absorption spectra of 10 μM of compound **3** and of 10 μM of **MB** in the presence and absence of calf thymus (CT) DNA (380 μM bp CT DNA, 10 mM sodium phosphate buffer pH 7.0; Table 1, Fig. 1A and 1B). Dye–nucleotide base-stacking interactions give rise to bathochromic wavelength shifts and hypochromic absorption in the electronic spectra of most if not all DNA intercalators. To more easily detect these DNA-induced spectral changes, the negatively charged surfactant sodium dodecyl sulfate (SDS) was added to samples with no DNA in order to disrupt phenothiazine dimerization.[2] (Dimerization of phenothiazines produces a blue-shifted absorption band with respect to the absorption band of corresponding phenothiazine monomer.[2])

Under our experimental conditions, 10 μM solutions of compound **3** and of **MB** exhibited maxima at 615 nm and 664 nm in the absence of 1% SDS and 675 nm ($\varepsilon = 1.45 \times 10^5$ M^{-1} cm^{-1}) and 661 nm ($\varepsilon = 7.84 \times 10^4$ M^{-1} cm^{-1}) in the presence of 1% SDS, respectively (Table 1, Fig. 1A and 1B). Thus, SDS produced a pronounced red shift only upon its addition to compound **3**, indicating that 10 μM of **3** undergoes extensive dimerization in the absence of the surfactant. Notwithstanding, when the 1% SDS was removed and then replaced with 380 μM bp CT DNA, bathochromic wavelength shifts and hypochromic absorption were generated, indicating that compound **3** dimerization was disrupted and that compound **3** and **MB** were bound to DNA under the experimental conditions employed: in the presence of the CT DNA, 10 μM of compound **3** and of **MB** exhibited maxima at 680 nm ($\varepsilon = 7.78 \times 10^4$ M^{-1} (bp) cm^{-1}) and 675 nm ($\varepsilon = 5.80 \times 10^4$ M^{-1} (bp) cm^{-1}), respectively. When the series of experiments was conducted using 1 μM of compound **3** and of **MB**, the corresponding UV–visible spectra exhibited the same general dimerization and DNA binding trends observed at 10 μM concentrations of phenothiazine (Fig. S1 in ESI†).

A previous comparison of **MB** to partially methylated analogs demonstrated that phenothiazine absorption moves to longer wavelengths as the degree of *N*-methylation increases (**MB** > azure B > azure A > azure C).[11,12] The electronic spectra of compound **3** and methylene blue in 1% SDS show that the effect of replacing an *N,N*-dimethyl group in **MB** with an electron donating ethylenedipiperidine linker is to induce an additional bathochromic wavelength shift. In the presence of either DNA or

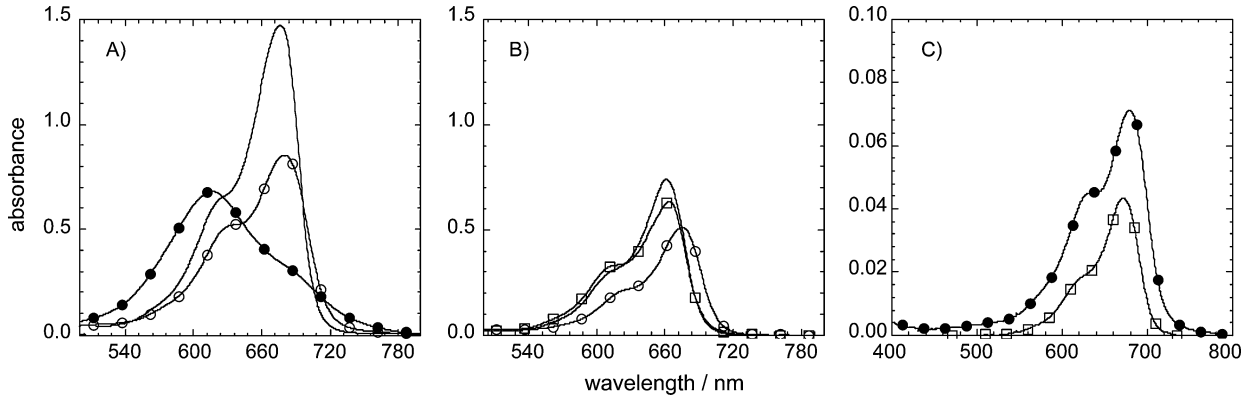

Fig. 1 UV–visible spectra recorded at 22 °C in 10 mM sodium phosphate buffer pH 7.0 of: (a) 10 μM compound **3** (●, λ_{max} = 615 nm) in the presence of 380 μM bp CT DNA (○, λ_{max} = 680 nm) or 1% SDS (w/v) (solid line, λ_{max} = 675 nm); (b) 10 μM **MB** (□, λ_{max} = 664 nm) in the presence of 380 μM bp CT DNA (○, λ_{max} = 675 nm) or 1% SDS (w/v) (solid line, λ_{max} = 661 nm); (c) 1 μM compound **3** (●, λ_{max} = 680 nm) or 1 μM MB (□, λ_{max} = 671 nm) with 38 μM bp CT DNA. Line markers (●,○,□) are placed at every 50th data point. Prior to data acquisition, the samples containing DNA were pre-equilibrated for 12 h in the dark at 22 °C.

SDS, it is evident that compound **3** absorbs light more strongly and at longer wavelengths in comparison to **MB** (Fig. 1A and 1B).

Photocleavage experiments

DNA photocleavage as a function of wavelength (676, 700 and 710 nm) and time (10, 30, 60 min) was studied next. Reactions were carried out in 10 mM sodium phosphate buffer pH 7.0 with 38 μM bp pUC19 plasmid DNA and 1 μM of **3** or **MB**. The samples were aerobically irradiated using a 75 W xenon lamp fitted with a monochromator. DNA photocleavage products were then visualized on a 1% nondenaturing agarose gel. While both phenothiazines showed time-dependant photocleavage that continued to increase after 30 min of irradiation, compound **3** exhibited markedly higher levels of cleavage at all time points and all wavelengths tested (Fig. 2). In Fig. 1C are the corresponding absorption spectra of compounds **3** and of **MB** prior to irradiation (10 mM sodium phosphate buffer pH 7.0 with 38 μM bp calf thymus DNA and 1 μM of each phenothiazine). The absorption of DNA-bound compound **3** is stronger and more red-shifted than DNA-bound **MB** at all three wavelengths (676, 700 and 710 nm in Fig. 1C, Table S1 in ESI†). Therefore, the absorbance data are in good general agreement with the higher levels of DNA photocleavage produced by 1 μM of compound **3** in comparison to 1 μM of **MB**.

We then used the longest wavelength in the series to compare DNA photocleavage as a function of dye concentration. (Due to the presence of hemoglobin and melanin, the main chromophores in human tissue, the penetration depth of visible light increases with increasing wavelength, and is higher at 710 nm in comparison to 676 nm and 700 nm.[1c,16]) Reactions consisting of 38 μM bp pUC19 plasmid DNA and 10 to 0.25 μM of compound **3** or **MB** were irradiated at 710 nm for 60 min. As shown in Fig. 3, compound **3** consistently generated higher levels of DNA photocleavage at all six tested concentrations. Notably, irradiation of only 5 μM of dye at 710 nm produced cleavage yields of 93% and 59% for **3** and **MB**, respectively. In addition, the cleavage levels produced by 5 to 0.5 μM concentrations of compound **3** were higher than the cleavage produced using greater to or equal than twice the concentrations of **MB** (10 to 1 μM). For example,

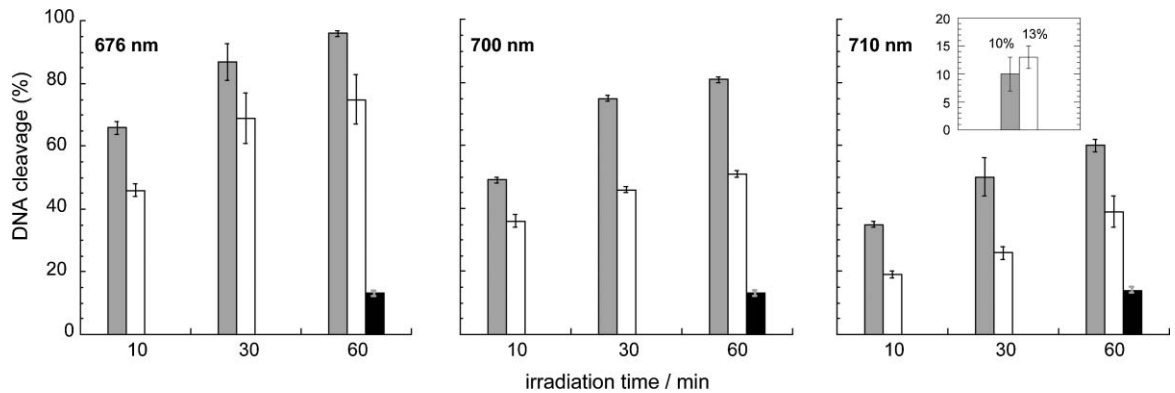

Fig. 2 % DNA photocleavage of 38 μM bp pUC19 plasmid DNA in the presence of 1 μM compound **3** (grey bars) or 1 μM **MB** (white bars) in 10 mM sodium phosphate buffer pH 7.0 at 22 °C. The samples were irradiated at 676, 700, or 710 nm with a 75 W xenon lamp connected to a monochromator. The black bars represent DNA that was irradiated for 60 min in 10 mM sodium phosphate buffer pH 7.0 in the absence of dye. In the inset are dark controls in which 1 μM of **3** and 1 μM of **MB** were treated with 38 μM bp pUC19 plasmid for 60 min (22 °C, no hv). % DNA cleavage (% nicked +% linear DNA) was averaged over three trials with error bars representing standard deviation.

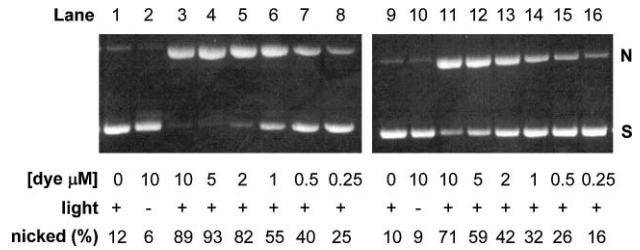

Fig. 3 Photograph of a 1% nondenaturing agarose gel showing photocleavage of pUC19 plasmid DNA. Samples contained 10 mM sodium phosphate buffer pH 7.0 and 38 μM bp DNA in the presence and absence of dye. After being equilibrated for 12 h in the dark at 22 °C, the samples were aerobically irradiated at 710 nm for 60 min at 22 °C. Lanes 1 and 9: DNA controls (no dye). Lanes 3 to 8: 10 to 0.25 μM compound **3**. Lanes 11 to 16: 10 to 0.25 μM **MB**. Lanes 2 and 10: 10 μM **3** and 10 μM **MB** (no hν). Abbreviations: N = nicked; S = supercoiled. It is evident that DNA photocleavage yields increase as a function of increasing dye concentration with one exception. We attributed the slight decrease in photocleavage observed in the presence of 10 μM of compound **3** to DNA precipitation.

710 nm irradiation cleaved plasmid DNA in 93% and 71% yields in the presence of 5 μM of **3** and 10 μM of **MB** and in 82% and 59% yields in the presence of 2 μM of **3** and 5 μM of **MB**.

Chemically induced changes in photocleavage

DNA photodamage by **MB** is thought to proceed primarily through a Type II (energy transfer) pathway in which singlet oxygen ($^1O_2$) produces the alkaline labile lesion 8-hydroxy-2-deoxy guanosine *ca.* 17 times more frequently than direct strand breaks.[17] We therefore conducted a series of experiments to test for the relative participation of singlet oxygen ($^1O_2$) compared to DNA damaging Type I hydroxyl radicals (·OH) in direct strand break formation. A total of 50 mM of the $^1O_2$ scavenger sodium azide or of the ·OH scavenger D-mannitol was added to photolysis reactions containing 1 μM of compound **3** or 1 μM of **MB** and 38 μM bp plasmid DNA (10 mM sodium phosphate pH 7.0). DNA photocleavage yields in the presence of sodium azide and D-mannitol were reduced by approximately 48% and 20% in reactions containing compound **3** and by 40% and 20% in reactions with **MB** (Table 2). These data indicate that singlet oxygen is likely to be a principal reactive species involved in phenothiazine-induced DNA photocleavage. Because deuterium oxide is known to increase the lifetime of singlet oxygen, an additional set of reactions was conducted in 85% D_2O (v/v). As shown in Table 2, the effect of this chemical was to increase phenothiazine cleavage yields by approximately 20%, supporting the involvement of $^1O_2$ in photoinduced DNA strand scission. Interestingly, the weak inhibitory effects of D-mannitol indicate that hydroxyl radicals may make a minor contribution. This latter result contrasts with a previous report in which hydroxyl radical scavengers were shown to be ineffective in inhibiting the production of methylene blue-sensitized direct strand breaks.[17]

Table 2 Percent change in DNA photocleavage by compound **3** and **MB** in the presence of scavengers and D_2O[a]

Compound	D-Mannitol	NaN_3	D_2O
3	−20 ± 1	−48 ± 2	+20 ± 6
MB	−20 ± 7	−40 ± 1	+20 ± 5

[a] Individual solutions consisted of 38 μM bp pUC19 plasmid DNA, 1 μM compound **3** or 1 μM **MB**, and 10 mM sodium phosphate buffer pH 7.0 in the presence of either 50 mM D-mannitol, 50 mM sodium azide (NaN_3), or 85% (v/v) D_2O. The solutions were aerobically irradiated at 710 nm for 60 min, 22 °C. Percent change in DNA photocleavage was averaged over three trials with errors reported as standard deviation.

DNA photocleavage at nucleotide resolution

To further investigate mechanism(s) underlying photocleavage, pUC19 plasmid DNA was linearized with *Eco*RI, 3′-end labeled with [^{35}S]dATPαS, and cut with *Fsp*I to generate a 138 bp restriction fragment. Duplicate sets of reactions containing 15 μM bp of the radiolabeled DNA in 20 mM sodium phosphate buffer pH 7.0 without and with 5 μM of **3** and 5 μM of **MB** were irradiated for 60 min in a ventilated Rayonet Photochemical Reactor fitted with twelve 575 nm lamps (spectral output 400–650 nm). In order to produce DNA strand breaks at alkaline labile lesions, half of the reactions were treated with 1% piperidine (90 °C, 30 min) immediately after the 60 min irradiation period. Products were resolved adjacent to G, G + A, and T chemical sequencing reactions on a 10% denaturing polyacrylamide gel. Shown in Fig. 4 are photocleavage plots generated from a representative 40 bp sequence within the 138 bp radiolabeled DNA fragment. In the absence of piperidine, it is evident that many of the direct strand breaks produced by compound **3** and **MB** are at guanine bases (Fig. 4A). This result points to a photocleavage mechanism that involves either singlet oxygen and/or direct electron transfer from DNA nucleobases, as both pathways produce preferential DNA damage at guanines.[18] (With respect to electron transfer, guanine possesses the lowest oxidation potential out of the four bases.) It can also be concluded that hydroxyl radicals are less likely to have played a major role. These reactive oxygen species cleave DNA by abstracting hydrogen atoms from deoxyribose. Because sugar residues are present at every nucleotide position, hydroxyl radicals and other reagents which function by hydrogen atom abstraction tend to cleave at all nearby DNA sequences irrespective of base composition.[19] Thus, the cleavage patterns produced by compound **3** and **MB** are in agreement with the photocleavage data in Table 2. Both indicate that singlet oxygen, rather than hydroxyl radicals, makes a more significant contribution to the formation of DNA direct strand breaks.

As shown in Fig. 4B, levels of damage at guanine bases were dramatically increased after the DNA photolysis reactions were treated with piperidine. This result indicates that irradiation of **3** and **MB** contributed to the formation of alkaline labile lesions at guanine bases, either through the production of singlet oxygen and/or by direct electron transfer from DNA. Notwithstanding, the different photocleavage patterns obtained after piperidine treatment indicate that the two phenothiazines may bind to DNA at different sites. In comparison to **3**, the damage produced by **MB** at the eleven guanine bases in the 40 bp fragment is more evenly distributed. For example, compound **3** is more specific for cleavage at the 3′-G of the two 5′-GGG-3′ tracts contained in the fragment. This is in contrast to the DNA damage produced by direct electron transfer, where base radical cation migration forms piperidine labile lesions at the second base in 5′-GGG-3′ sequences.[20] Taken

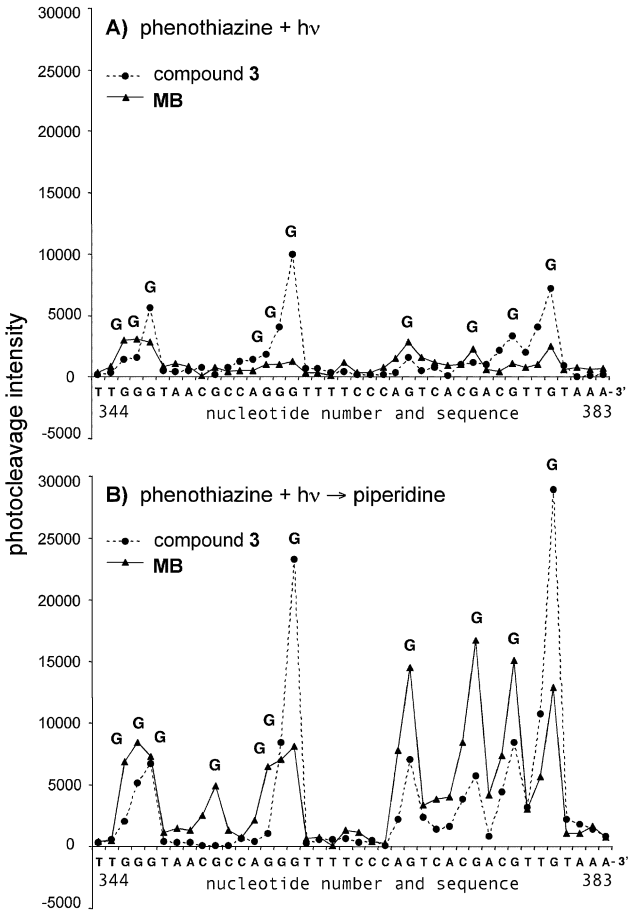

Fig. 4 Cleavage plots of a representative 40 bp DNA sequence. Photocleavage intensities as a function of base were calculated by quantitating a storage-phosphor autoradiogram of DNA photocleavage products resolved on a 10% denaturing polyacrylamide gel. A total of 15 μM bp of ^{35}S 3′-end labeled 138 bp restriction fragment was irradiated at 575 nm in the presence of 5 μM **3** and 5 μM **MB** without (a) and with (b) post-irradiation piperidine treatment.

together, the above data indicate that DNA binding by **3** is non-uniform in comparison to **MB** and that its photocleavage pattern might arise from locally higher concentrations of singlet oxygen at preferentially bound DNA sites.[21] Our results are in agreement with previously published work in which the majority of direct strand breaks and alkaline labile lesion produced by irradiation of **MB** occurred at guanine bases.[17,22]

Thermal denaturation

Thermal melting studies offer a reliable method for ranking the relative affinities of ligands that preferentially bind to helical forms of DNA. In the process of intercalation and/or groove binding, favorable free energy contributions arising from π–π, van der Waals, electrostatic, and hydrogen bonding interactions increase the DNA binding affinity of these ligands, and stabilize the DNA duplex. Because more heat energy must be applied to melt the ligand-bound duplex, the melting temperature (T_m) of the DNA is increased.[23] We recorded thermal melting curves at dye to DNA bp molar ratios (r = [dye]/[DNA bp]) ranging from 0.05 to 0.6 (12.5 μM bp CT DNA in 10 mM sodium phosphate buffer pH 7.0). While the ΔT_m values produced by **MB** continued to increase, the ΔT_m values produced by **3** remained constant at $r \geq 0.3$, indicating that DNA saturation by this compound had been reached (Fig. 5A). Shown in Fig. 5B are the corresponding

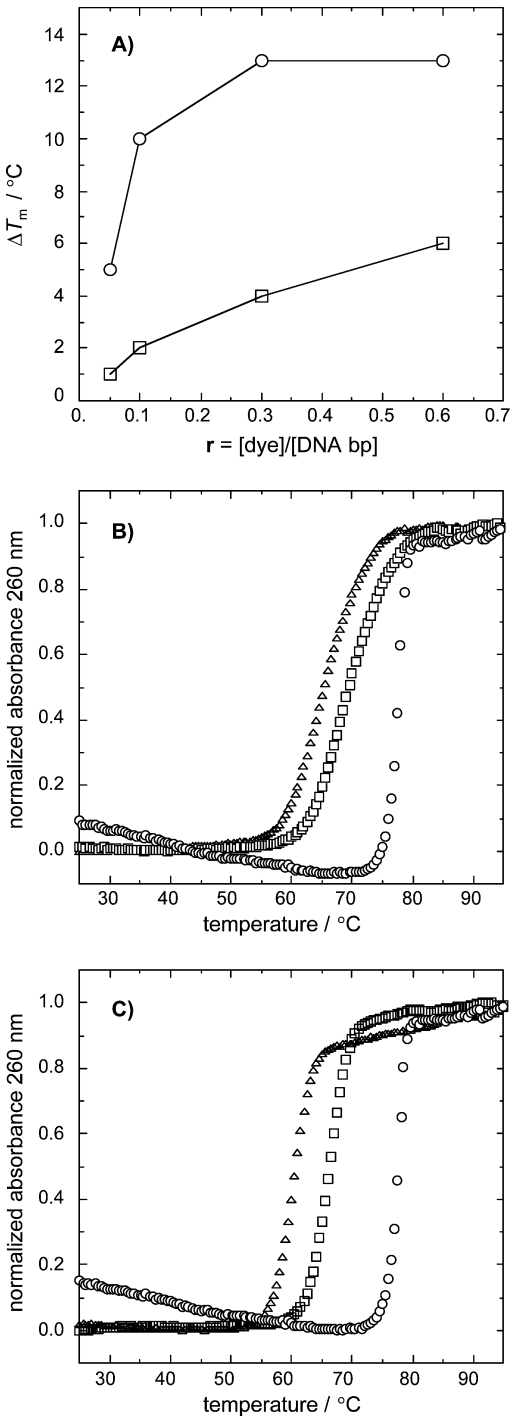

Fig. 5 (a) ΔT_m values of 12.5 μM bp CT DNA in 10 mM sodium phosphate buffer pH 7.0 and 0.625, 1.25, 3.75, and 7.50 μM of phenothiazine: ○ = **3**, □ = **MB**. (b) Thermal melting curves of: 12.5 μM bp CT DNA (Δ, T_m = 65 °C), 12.5 μM bp CT DNA and 3.75 μM of **MB** (□, T_m = 69 °C), or 3.75 μM of **3** (○, T_m = 78 °C). (c) Melting curves of: 12.5 μM bp CP DNA (Δ, T_m = 60 °C), 12.5 μM bp CP DNA and 3.75 μM of **MB** (□, T_m = 66 °C), or 3.75 μM of **3** (○, T_m = 78 °C).

melting curves generated at r values of 0.0 and 0.3. Under these conditions, the melting temperature (T_m) obtained for CT DNA was 65 °C, while the addition of compound **3** or **MB** produced T_m values of 78 °C (ΔT_m = 13 °C) and 69 °C (ΔT_m = 4 °C), respectively. When the ratio of dye to DNA bp was doubled from 0.3 to 0.6, the T_m for **MB** was 71 °C (ΔT_m = 6 °C), still significantly lower than the T_m of 78 °C (ΔT_m = 13 °C), recorded for compound **3** at saturation (r = 0.3 and 0.6). Even at the lowest ratio in the series (r = 0.05), the addition of **3** raised the T_m of CT DNA from 65 °C to 70 °C, compared to only 66 °C for **MB**.

In order to rank the relative DNA binding affinities of compound **3** and **MB** as a function of DNA sequence, we recorded additional melting isotherms using *C. perfringens* DNA (CP DNA; 12.5 μM bp CP DNA in 10 mM sodium phosphate buffer pH 7.0). In comparison to CT DNA (58% AT), CP DNA possesses a higher AT content (69%). As shown in Fig. 5C, the T_m of CP DNA is 60 °C, while the addition of **3** or **MB** at an r value of 0.3 raises the T_m to 78 °C (ΔT_m = 18 °C) and 66 °C (ΔT_m = 6 °C), respectively.

Collectively, the CT and CP DNA melting data indicate that compound **3** produces an approximately three fold higher level of duplex stabilization compared to **MB** under identical experimental conditions: at r = 0.3, the ΔT_m values of 12.5 μM bp of CT and CP DNAs were 13 °C and 18 °C for **3** and 4 °C and 6 °C for **MB**. Thus, higher DNA binding affinity in addition to stronger light absorption may account for the ability of compound **3** to photocleave DNA more efficiently. Because compound **3** and **MB** generated higher ΔT_m values in the presence of CP DNA compared to CT DNA, interaction of these phenothiazines with AT rich sequences is likely to stabilize the nucleic acid duplex to a greater degree than their interaction with GC rich sequences. Finally, the T_m data indicate that compound **3** saturates CT DNA binding sites at a significantly lower concentration than **MB**. It can be inferred from this latter result that either the linker chain and/or the second phenothiazine ring of **3** may come into direct contact with DNA.

Viscometric measurements

Viscosity provides a simple and stringent hydrodynamic assay for inferring the binding modes of DNA interacting compounds in the absence of X-ray crystallography and/or high-resolution NMR structural data. When an intercalator binds to duplex DNA, the helix unwinds and lengthens to accommodate the ligand in between base pairs. This increase in length results in an increase in DNA viscosity. Alternatively, groove binding compounds do not lengthen helical DNA and viscosity is not significantly changed.[24] In the case of classical monointercalators such as daunomycin, ethidium bromide, and proflavin, the slopes observed from plots of the cubed root of the relative viscosity ($(\eta/\eta_o)^{1/3}$) *versus* r (molar ratio of bound ligand to DNA bp) range from 0.80 to 1.50.[25] For bisintercalators, typical slopes are from 1.3 to 2.3.[25c,26]

Fig. 6 shows that viscometric data of **MB** with CT DNA (42% GC) yields a slope of 0.962 ± 0.002, clearly consistent with monofunctional intercalation, while the slope for compound **3** is 1.50 ± 0.13 and is within the ranges expected for both mono- and bisintercalators. Notwithstanding, **3** increases the viscosity of CT DNA to a significantly greater extent than **MB** (Fig. 6), leading us to hypothesize that the association of compound **3** with DNA might involve the existence of multiple binding modes (*e.g.*, concomitant monointercalation, bisintercalation, and/or groove binding). In fact, combinations of these modes are thought to account for DNA viscosity enhancements produced by a number of bifunctional agents with non-ideal slopes (usually lower than twice the slope of the corresponding monointercalator).[27]

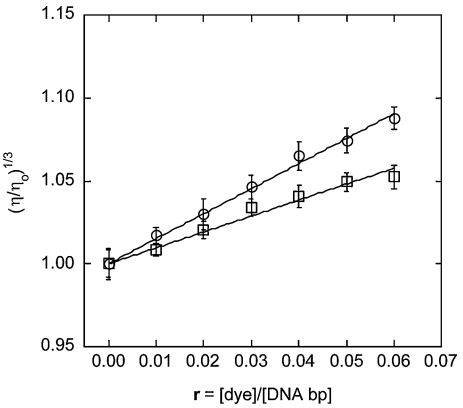

Fig. 6 Viscometric measurements of CT DNA in the presence of compound **3** (○, slope = 1.50 ± 0.130, R = 0.997) and **MB** (□, slope = 0.962 ± 0.002, R = 0.987). The values were averaged over at least three trials. Error bars represent standard deviation.

To test our hypothesis, we performed viscometric measurements of **3** and **MB** in the presence of additional double-helical sequences. Plots of $(\eta/\eta_o)^{1/3}$ *versus* r for poly(dA)·poly(dT) and alternating poly[(dA-dT)]$_2$ DNAs yielded slopes of 0.22 and 1.18 for compound **3**, and 0.17 and 1.11 for **MB**, respectively (Fig. S7 in ESI†). These data indicate the existence of different binding modes as a function of DNA sequence: groove binding for poly(dA)·poly(dT) and monointercalation for poly[(dA-dT)]$_2$. However, taking into consideration the minimal effect of compound **3** on poly(dA)·poly(dT) viscosity, we recorded the circular dichroism (CD) spectra shown in Fig. 7. The strong, positive induced CD signal at 690 nm confirms the formation of a complex in which **3** associates with the DNA duplex *via* groove binding.

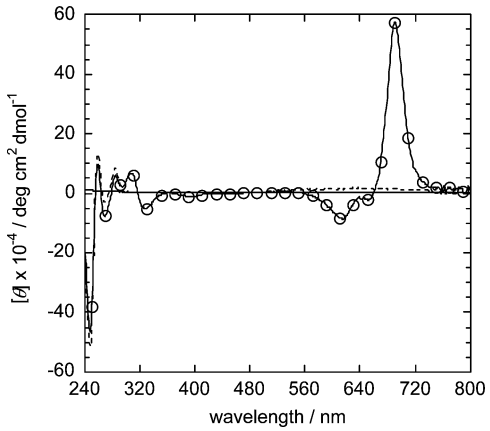

Fig. 7 CD spectra recorded at 22 °C of 10 mM sodium phosphate buffer pH 7.0 in the presence and absence of 50 μM bp poly(dA)·poly(dT) DNA or 12 μM of compound **3**. Solid line: compound **3**. Dashed line: poly(dA)·poly(dT) DNA. ○: compound **3** + poly(dA)·poly(dT) DNA (○ line marker is placed at every 20th data point).

The above viscosity data are consistent with a published CD study in which **MB** was shown to bind to poly(dA)·poly(dT) and

Table 3 Viscometric data[a]

	Slope	
Deoxyribonucleic acid	**MB**	Compound **3**
poly(dA)-poly(dT)	0.17	0.22
$[poly(dAdT)]_2$	1.11	1.18
CT DNA (58% AT)	0.92	1.50

[a] The slopes of viscometric plots of the cubed root of relative DNA viscosity ($(\eta/\eta_o)^{1/3}$) *versus r*, molar ratio of bound ligand (**MB** or compound **3**) to DNA bp.

alternating poly[(dA-dT)]$_2$ by groove binding and intercalation, respectively.[28] The same study provided convincing evidence that **MB** interacts with poly(dG)·poly(dC) by intercalation. We next attempted to measure the viscosity of poly(dG)·poly(dC) and *M. lysodeikticus* (28% AT) DNA, but were unsuccessful due to DNA precipitation in the presence of high concentrations of **3**. Notwithstanding, when the poly(dA)·poly(dT), alternating poly[(dA-dT)]$_2$, and CT DNA (58% AT) slopes are compared side by side (Table 3), it can be inferred that CT DNA interacts with **MB** by groove binding and monofunctional intercalation, and with compound **3** by a combination of three modes: groove binding, and mono- and bisintercalation.

Conclusion

We have synthesized a new DNA photocleaving agent (**3**) in which two phenothiazine units are attached by an ethylenedipiperidine linker. To the best of our knowledge, compound **3** represents the first example of a phenothiazine that binds to DNA through bisintercalation. In comparison to the parent phenothiazine methylene blue, this compound absorbs light more strongly at longer wavelengths, exhibits higher levels of photocleavage under near physiological conditions of temperature and pH, and, as indicated by T_m data, associates more strongly with double-helical DNA. Our future research efforts will focus on obtaining high-resolution structural data that will aid in the design of new and effective DNA intercalators. We envisage that phenothiazine-based compounds will represent attractive alternatives to porphyrins for use in phototherapeutic applications.

Experimental

General materials and methods

Merck silica gel 60 (230–400 ASTM mesh) was employed for flash column chromatography. TLC was performed on precoated aluminium silica gel plates (Merck or Macherey-Nagel 60F254 0.25 mm). Melting points were determined in a Stuart Scientific model SMP10 apparatus. Infrared spectra were taken on an FT-IR Perkin Elmer Spectrum One spectrophotometer. ^{1}H and ^{13}C NMR spectra were recorded at 300 and 75 MHz, respectively, on either Varian Unity One or Varian Mercury-VX-300 spectrometers. Carbon and proton assignments were based on HSQC, HMBC, and HMQC spectra obtained using a Varian Unity Plus 500 MHz instrument. Tetramethylsilane was utilized as an internal reference. Coupling constants (*J* values) are given in Hz. Electrospray ionization (ESI) mass spectra were acquired on a Micromass Q-Tof hybrid mass spectrometer. Elemental analyses (CHNS) were done on a Leco CHNS-932 automatic analyzer. Iodine composition was performed by oxygen flask combustion and by ion chromatography (Atlantic Microlabs, Inc. Norcross, GA). UV–visible and CD spectra were recorded with a UV-1601 Shimadzu spectrophotometer and a JASCO J-810 spectropolarimeter, respectively. Thermal melting curves were generated using a Cary Bio100 UV–visible spectrophotometer.

Distilled, deionized water was utilized in the preparation of all buffers and aqueous reactions. Chemicals were of the highest available purity and were used without further purification. Methylene blue chloride (99.99% purity) was purchased from Fluka. Caesium carbonate, chloroform, D_2O, dimethylamine (2 M solution in methanol), DMF, ethidium bromide, 4,4′-ethylenedipiperidine dihydrochloride, iodine, 10*H*-phenothiazine, sodium azide, sodium benzoate, sodium phosphate dibasic, and sodium phosphate monobasic were obtained from the Aldrich Chemical Co. Transformation of *Escherichia coli* competent cells (Stratagene, XL-blue) with pUC19 plasmid (Sigma) and growth of bacterial cultures in Lauria-Bertani broth were performed according to standard laboratory procedures.[29] The plasmid DNA was purified with a Qiagen Plasmid Mega Kit. The restriction enzymes *Eco*RI and *Fsp*I were purchased from New England BioLabs and [^{35}S]dATPαS was supplied by GE Healthcare. Ultra Pure™ calf thymus (Invitrogen Lot No. 15633–019, 10 mg mL^{-1}, average size ≤ 2000 bp) and *C. perfringens* DNA (Sigma, Lot No. 024K4065, purity ratio A_{260}/A_{280} = 1.9) were used without purification. The DNA polymers poly(dA)·poly(dT) (average size ~6000 bp, Lot No. GD0276), and poly[(dA-dT)]$_2$ (average size ~5183 bp, Lot No. GF0106) were obtained as lyophilized powders from Amersham Biosciences. They were dissolved in 10 mM sodium phosphate pH 7.0 and were used without further purification. The concentrations of all DNA solutions were determined by UV–visible spectrophotometry using the following extinction coefficients in units of dm^3 mol^{-1} (bp) cm^{-1}: calf thymus DNA, ε_{260} = 12 824; *C. perfringens* DNA, ε_{260} = 12 476; poly(dA)·poly(dT), ε_{260} = 12 000; and poly[(dA-dT)]$_2$, ε_{262} = 13 200.

N,*N*′-Bis[(7-dimethylamino)phenothiazin-5-ium-3-yl]-4,4′-ethylenedipiperidine diiodide (3)

To a solution of **2** (0.200 g, 0.322 mmol) in 20 mL of DMF were added 4,4′-ethylenedipiperidine dihydrochloride (0.044 g, 0.161 mmol) and caesium carbonate (0.629 g, 1.931 mmol). The reaction was vigorously stirred at rt for 48 h and then concentrated under reduced pressure. The progress of the reaction was monitored by silica gel TLC (9.5 : 0.5 dichloromethane–methanol). The resultant solid was purified by flash column chromatography (3 cm column, 39 g silica gel) using 9.5 : 0.5 dichloromethane–methanol as the eluent. Then, two successive recrystallizations from methanol afforded dark-blue solid **3** (81 mg, 54%), mp > 300 °C (from MeOH); R_f = 0.2 (9.5 : 0.5 dichloromethane–methanol); ν_{max} (film)/cm^{-1} 2907, 1592, 1487, 1389, 1330, 1232, 1133, 1038, 969, 883, 825, and 779; δ_H(300 MHz, 4 : 6 $CDCl_3$–CD_3OD; Me_4Si) 7.95 (2H, d, *J* 9.6, H-1), 7.94 (2H, d, *J* 9.6, H-9), 7.50–7.46 (4H, m, H-6, H-8), 7.33 (2H, dd, *J* 9.6 and 2.7, H-2), 7.26 (2H, d, *J* 2.7, H-4), 4.42 (4H, d, *J* 13.5, 2 × CH_2-α), 3.43 (12H, s, 2 × N(CH_3)$_2$), 3.38 (4H, m, overlap with CH_3OH, 2 × CH_2-α), 2.06 (4H, d, *J* 11.7, 2 × CH_2-β), 1.81 (2H, broad, 2 × C*H*) and 1.44–1.31 (8H, m, CH_2-CH_2, 2 × C*H*-β); δ_C(75 MHz, 4 : 6 $CDCl_3$–CD_3OD;

Me_4Si) 154.3 and 153.3 (C-3, C-7), 139.2 and 138.7 (C-1, C-9), 136.4, 135.9, 135.8, and 134.8 (C4a, C5a, C9a and C10a), 119.3 and 118.6 (C-2, C-8), 107.1 and 106.4 (C-4, C-6), 49.3 (C-α), 41.6 (NCH_3), 35.8 (CH), 33.0 and 32.9 (C-β, CH_2-CH_2); *m/z* (HR-ESI) 337.1612 ($M^{2+} - C_{40}H_{46}N_6S_2$ requires 337.1613).

UV–visible spectrophotometry

Extinction coefficients for compound **3** and **MB** were determined using 500 μL solutions containing 1 to 10 μM of dye in the presence and absence of 38 to 380 μM bp calf thymus DNA in 10 mM sodium phosphate buffer pH 7.0. The solutions were pre-equilibrated for 12 h in the dark, after which spectra were recorded in 1 cm quartz cuvettes at 22 °C. The absorbance was then plotted as a function of concentration and linear least square fits to these data yielded slopes (KaleidaGraph version 3.6.4 software) that were averaged over three trials. Using the procedure described above, extinction coefficients in the absence of calf thymus DNA were also recorded in the presence of a final concentration of aqueous 1% sodium dodecyl sulfate (w/v).

Photocleavage experiments

Individual samples consisted of 38 μM bp pUC19 plasmid DNA and 10 to 0 μM of compound **3** or **MB** in 10 mM sodium phosphate buffer pH 7.0 (total volume 20 μL). The samples were pre-equilibrated in the dark for 12 h at 22 °C, after which they were kept in the dark or aerobically irradiated at 676, 700 or 710 nm for 10, 30, or 60 min at 22 °C using a Photon Technology Inc. Model A1010 light supply fitted with a 75 W xenon lamp and a monochromator with a grating (blazed at 500 nm, 1200 lines/mm, 20 nm slit width). After irradiation, cleavage products were electrophoresed on a 1% nondenaturing agarose gel stained with ethidium bromide (0.5 μg mL^{-1}), visualized on a transilluminator set at 302 nm, photographed, and scanned. The amounts of supercoiled, nicked, and linear plasmid DNA were quantitated by densitometry using ImageQuant version 5.2 software (Amersham Biosciences). Photocleavage yields were calculated using the formula [(nicked DNA + linear DNA)/total DNA] × 100. The density of supercoiled DNA was multiplied by a correction factor of 1.22 to account for the decreased binding affinity of ethidium bromide to supercoiled DNA as compared to the nicked and linear forms. Photocleavage concentration profiles were conducted as described above. In these experiments, individual reactions consisting of 10 to 0.0 μM of compound **3** or of **MB** in the presence of 38 μM bp pUC19 plasmid DNA were irradiated at 710 nm for 60 min.

Chemically induced changes in DNA photocleavage

Immediately prior to irradiation, a chemical additive, either sodium azide (final concentration 50 mM), D-mannitol (final concentration 50 mM), or D_2O (final concentration 85% (v/v)) was transferred to individual 20 μL reactions consisting of 38 μM bp pUC19 plasmid DNA pre-equilibrated with 1 μM of compound **3** or **MB** in 10 mM sodium phosphate buffer pH 7.0 in the dark for 12 h at 22 °C. Control reactions containing 1 μM of compound **3** or **MB**, 38 μM bp pUC19 plasmid, and 10 mM sodium phosphate buffer pH 7.0 were run in which an equivalent volume of ddH_2O was used to substitute for the sodium azide, D-mannitol, or D_2O. The samples were then aerobically irradiated at 710 nm using a Photon Technology Inc. light supply (Model A1010) fitted with a 75 W xenon lamp and monochromator with a grating (blazed at 500 nm, 1200 lines/mm, 20 nm slit width) for 60 min at 22 °C. Reaction products were resolved on a 1% nondenaturing agarose gel and quantitated as described above. The percent change in DNA photocleavage was calculated as follows: [((% cleavage with chemical) − (% cleavage without chemical))/(% cleavage without chemical)] × 100.

DNA photocleavage at nucleotide resolution

An established laboratory protocol was used to prepare a 138 bp *Eco*RI-*Fsp*I pUC19 restriction fragment 3′-end-labeled with [^{35}S]dATPαS.[30] The purified, radiolabeled DNA was stored at −78 °C in a total volume of 400 μL of ddH_2O until use.

Typical photocleavage reactions contained 15 μM bp of the 138 bp DNA fragment in 10 mM sodium phosphate buffer pH 7.0 and 5 μM of **3** or 5 μM of **MB** (50 μL total volume). The reactions were pre-equilibrated in the dark at 22 °C for 2 h and then were aerobically irradiated for 60 min in a ventilated Rayonet Photochemical Reactor (Southern New England Ultraviolet Co.) fitted with twelve 575 nm lamps (spectral output 400–650 nm). The photolyzed DNA was precipitated with 40 μg glycogen–2.5 volumes neat ethanol, and washed with 70% aqueous ethanol. A duplicate set of precipitated reactions was dissolved in 100 μL of 1% aqueous piperidine, heated at 90 °C for 30 min, and then lyophilized to dryness. Cleavage products without and with piperidine treatment were dissolved in 4 μL of Sequenase™ Stop Solution, denatured for 3 min at 95 °C, and then electrophoresed on a 10% denaturing polyacrylamide gel adjacent to G, G + A, and T chemical sequencing reactions.[30a] To determine yields, the gel was scanned with a Storm 860 PhosphorImager (Molecular Dynamics). The resulting storage-phosphor autoradiogram was quantitated using ImageQuant 5.2 software (Molecular Dynamics).

Thermal melting studies

Individual 3 mL solutions containing 10 mM sodium phosphate buffer pH 7.0 and 12.5 μM bp calf thymus DNA in the presence and absence of 0.625, 1.25, 3.75 and 7.50 μM of compound **3** or of **MB** were placed in 3 mL (1 cm) quartz cuvettes (Starna). Similarly, 12.5 μM bp *C. perfringens* DNA was utilized in the presence and absence of 3.75 μM of compound **3** or **MB**. After the samples were equilibrated in the dark for 12 h and 22 °C, absorbance was monitored at 260 nm while the DNA was denatured using a Peltier heat block programmed to increase the temperature from 25 to 95 °C at a rate of 0.5 °C min^{-1}. KaleidaGraph version 3.6.4 software was then used to approximate the first derivative of $\Delta A_{260}/\Delta T$ *versus* temperature. The T_m values were determined according to the maximum of each first derivative plot.

Viscosity measurements

In a total volume of 1 mL, individual solutions containing 10 mM sodium phosphate buffer pH 7.0 and 200 μM bp of calf thymus DNA (average length ≤2000 bp) in the absence and presence of 2 to 12 μM of compound **3** or **MB** were pre-equilibrated for 12 h in the dark at 22 °C. DNA viscosity was then measured in a

Cannon-Ubbelohde size 75 capillary viscometer immersed in a thermostated water bath maintained at 25 ± 0.1 °C. The flow times of the buffer, DNA in buffer, and dye–DNA in buffer were measured with a stopwatch. The measurements were averaged over four trials to an accuracy of ±0.2 s. After subtracting the averaged flow time of the buffer, DNA (η_0) and dye–DNA (η) averaged flow times were plotted as $(\eta/\eta_o)^{1/3}$ *versus* the molar ratio of dye to DNA bp.[31] Slopes were generated by conducting linear least square fits to these data (KaleidaGraph version 3.6.4 software). The viscosity measurements containing poly(dA)·poly(dT) (average length ~6000 bp) and poly[(dA-dT)]$_2$ (average length ~5183 bp) were done exactly as described for calf thymus DNA except that DNA concentrations were decreased to account for the longer average lengths of these polymers compared to calf thymus DNA. Accordingly, measurements were conducted with 50 μM bp of each polymer and 0.5 to 3 μM of compound **3** or **MB** (Fig. S7 in ESI†) such that dye to DNA bp molar ratios were consistent with the calf thymus DNA measurements. While the conventional method for performing viscosity assays involves titration of the ligand into a DNA solution inside the viscometer, here we report an alternative and efficient technique that may be particularly useful for **3** as well as for other phenothiazines (*e.g.*, 1,9-dimethyl methylene blue and methylene blue) where pre-equilibration with DNA is required to reduce ligand self-stacking interactions in solution.[32]

Circular dichroism analysis

Samples consisted of 10 mM sodium phosphate buffer pH 7.0 and 12 μM of compound **3** in the presence and absence of 50 μM bp poly(dA)·poly(dT) DNA in a total volume of 500 μL. After equilibration in the dark for 12 h at 22 °C, spectra were recorded from 800 to 200 nm at 22 °C in a 0.5 cm quartz cuvette using a scan rate of 100 nm min^{-1} and a time constant of 1 s. The spectra were averaged over 4 acquisitions and were baseline-corrected to remove signals generated by the buffer.

Acknowledgements

This work was supported by the NSF (CHE-9984772; K.B.G), the CICYT (Project BQU 2002–02576; A.L.) and the US Department of Education (GAANN Fellowship; B.W.). We are grateful for assistance from Profs M.W. Germann, T.L. Netzel, L. Strekowski, W.D. Wilson, and Dr C. Sekar (GSU); and from Dr M.V. Galakhov (UAH).

References

1 (*a*) S. Pervaiz and M. Olivo, *Clin. Exp. Pharmacol. Physiol.*, 2006, **33**, 551–556; (*b*) M. A. Awan and S. A. Tarin, *Surgeon*, 2006, **4**, 231–236; (*c*) J. Juzeniene and A. Moan, *Photodiagn. Photodyn. Ther.*, 2007, **4**, 3–11.
2 J. P. Tardivo, A. Del Giglio, C. S. Oliveira, D. S. Gabrielli, H. C. Junqueira, D. B. Tada, D. Severino, R. F. Turchiello and M. S. Baptista, *Photodiagn. Photodyn. Ther.*, 2005, **2**, 175–191.
3 (*a*) K. Orth, D. Russ, G. Beck, A. Rück and H. G. Beger, *Langenbecks Arch. Surg.*, 1998, **383**, 276–281; (*b*) K. Orth, G. Beck, F. Genze and A. Rück, *J. Photochem. Photobiol., B*, 2000, **57**, 186–192.
4 (*a*) K. Orth, A. Rück, A. Stanescu and H. G. Beger, *Lancet*, 1995, **345**, 519–520; (*b*) J. P. Tardivo, A. Del Giglio, L. H. Paschoal and M. S. Baptista, *Photomed. Laser Surg.*, 2006, **24**, 528–531.
5 (*a*) B. Lambrecht, H. Mohr, J. Knuever-Hopf and H. Schmitt, *Vox Sang.*, 1991, **60**, 207–213; (*b*) M. Wainwright, D. A. Phoenix, S. L. Laycock, D. R. A. Wareing and P. A. Wright, *FEMS Microbiol. Lett.*, 1998, **160**, 177–181; (*c*) T. N. Demidova and M. R. Hamblin, *Proc. SPIE*, 2005, **5689**, 66–77; (*d*) J. F. Papin, R. A. Floyd and D. P. Dittmer, *Antiviral Res.*, 2005, **68**, 84–87; (*e*) M. Wainwright, H. Mohr and W. H. Walker, *J. Photochem. Photobiol., B*, 2007, **86**, 45–58.
6 (*a*) I. Fukui, M. Yokokawa, G. Mitani, F. Ohwada, M. Wakui, M. Washizuka, T. Tohma, K. Igarashi and T. Yamada, *J. Urol.*, 1983, **130**, 252–255; (*b*) I. Titley, R. N. Davidson, E. Turner, E. R. Hicks, N. T. Cooke, W. N. Landells and M. M. Levene, *Resp. Med.*, 1989, **83**, 37–41; (*c*) N. S. Magee and R. F. Wagner, *J. Am. Acad. Dermatol.*, 2004, **50**, 640–641.
7 (*a*) Y. Fukui, T. Yamakawa, T. Taniki, S. Numoto, H. Miki and Y. Monden, *Cancer*, 2001, **92**, 2868–2874; (*b*) K. Eldrageely, M. P. Vargas, I. Khalkhali, R. Venegas, M. Burla, K. D. Gonzalez and H. I. Vargas, *Am. Surg.*, 2004, **70**, 872–875.
8 (*a*) P. N. Patel, *Ann. Pharmacother.*, 2006, **40**, 299–303; (*b*) N. E. Camp, *J. Emerg. Nurs.*, 2007, **33**, 172–174.
9 (*a*) A. Rück, T. Köllner, W. S. Dietrich and H. Schneckenburger, *J. Photochem. Photobiol., B*, 1992, **12**, 403–412; (*b*) B. B. Noodt, G. H. Rodal, M. Wainwright, Q. Peng, R. Horobin, J. M. Nesland and K. Berg, *Int. J. Cancer*, 1998, **75**, 941–948.
10 R. G. Harris, J. D Wells and B. B. Johnson, *Colloids Surf., A*, 2001, **180**, 131–140.
11 E. M. Tuite and J. M. Kelly, *Biopolymers*, 1995, **35**, 419–433.
12 (*a*) E. M. Tuite and J. M. Kelly, *J. Photochem. Photobiol., B*, 1993, **21**, 103–124; (*b*) M. Wainwright, D. A. Phoenix, L. Rice, S. M. Burrow and J. Waring, *J. Photochem. Photobiol., B*, 1997, **40**, 233–239.
13 M. Delepierre, R. Maroun, C. Garbay-Jaureguiberry, J. Igolen and B. P. Roques, *J. Mol. Biol.*, 1989, **210**, 211–228.
14 L. Strekowski, D.-F. Hou and R. L. Wydra, *J. Heterocycl. Chem.*, 1993, **30**, 1693–1695.
15 (*a*) N. Leventis, M. Chen and C. Sotiriou-Leventis, *Tetrahedron*, 1997, **53**, 10083–10092; (*b*) K. J. Mellish, R. D. Cox, D. I. Vernon, J. Griffiths and S. B. Brown, *Photochem. Photobiol.*, 2002, **75**, 392–397.
16 (*a*) J. Eichler, J. Knof and H. Lenz, *Radiat. Environ. Biophys.*, 1977, **14**, 239–242; (*b*) P. Juzenas, A. Juzeniene, O. Kaalhus, V. Iani and J. Moan, *Photochem. Photobiol. Sci.*, 2002, **1**, 745–748; (*c*) K. P. Nielsen, A. Juzeniene, P. Juzenas, K. Stamnes, J. J. Stamnes and J. Moan, *Photochem. Photobiol.*, 2005, **81**, 1190–1194.
17 J. E. Schneider, S. Price, L. Maidt, J. M. C. Gutteridge and R. A. Floyd, *Nucleic Acids Res.*, 1990, **18**, 631–635.
18 (*a*) I. E. Kochevar and D. A. Dunn, in *Bioorganic Photochemistry*, ed. H. Morrison, Wiley, New York, 1990, vol. 1, pp. 273–315; (*b*) T. P. Devasagayam, S. Steenken, M. S. Obendorf, W. A. Schulz and H. Sies, *Biochemistry*, 1991, **30**, 6283–6289.
19 B. Armitage, *Chem. Rev.*, 1998, **98**, 1171–1200.
20 I. Saito, T. Nakamura, K. Nakatani, Y. Yoshioka, K. Yamaguchi and H. Sugiyama, *J. Am. Chem. Soc.*, 1998, **120**, 12686–12687.
21 H. Y. Mei and J. K. Barton, *Proc. Natl. Acad. Sci. U. S. A.*, 1988, **85**, 1339–1343.
22 C. OhUigin, D. J. McConnell, J. M. Kelly and W. J. M. van der Putten, *Nucleic Acids Res.*, 1987, **15**, 7411–7427.
23 W. D. Wilson, F. A. Tanious, M. Fernández-Saiz, in *Drug–DNA Interaction Protocols*, ed. K. R. Fox, Humana Press, New Jersey, 1997, pp. 219–240.
24 D. Suh and J. B. Chaires, *Bioorg. Med. Chem.*, 1995, **3**, 723–728.
25 (*a*) D. S. Drummond, N. J. Pritchard, V. F. W. Simpson-Gildemeister and A. R. Peacocke, *Biopolymers*, 1966, **4**, 971–987; (*b*) Y. Kubota, K. Hashimoto, K. Fujita, M. Wakita, E. Miyanohana and Y. Fujisaki, *Biochim. Biophys. Acta*, 1977, **478**, 23–32; (*c*) J. B. Chaires, F. Leng, T. Przewloka, I. Fokt, Y.-H. Ling, R. Perez-Soler and W. Priebe, *J. Med. Chem.*, 1997, **40**, 261–266.
26 (*a*) C.-H. Huang, S. Mong and S. T. Crooke, *Biochemistry*, 1980, **19**, 5537–5542; (*b*) W. D. Wilson, R. A. Keel, R. L. Jones and C. W. Mosher, *Nucleic Acids Res.*, 1982, **10**, 4093–4106; (*c*) P. Léon, C. Garbay-Jaureguiberry, B. Lambert, J. B. Le Pecq and B. P. Roques, *J. Med. Chem.*, 1988, **31**, 1021–1026; (*d*) J. A. Bordelon, K. J. Feirabend, S. A. Siddiqui, L. L. Wright and J. T. Petty, *J. Phys. Chem. B*, 2002, **106**, 4838–4843; (*e*) H.-L. Chan, D.-K. Ma, M. Yang and C.-M. Che, *J. Biol. Inorg. Chem.*, 2003, **8**, 761–769.
27 (*a*) B. Gaugain, J. Barbet, N. Capelle, B. P. Roques and J. B. Le Pecq, *Biochemistry*, 1978, **17**, 5078–5088; (*b*) L. P. G. Wakelin, M.

Romanos, T. K. Chen, D. Glaubiger, E. S. Canellakis and M. J. Waring, *Biochemistry*, 1978, **17**, 5057–5063; (*c*) D. Pelaprat, A. Delbarre, I. Le Guen, B. P. Roques and J. B. Le Pecq, *J. Med. Chem.*, 1980, **23**, 1336–1343; (*d*) W. A. Denny, G. J. Atwell, G. A. Willmott and L. P. G. Wakelin, *Biophys. Chem.*, 1985, **22**, 17–26; (*e*) N. W. McFayden, D. Sortirellis, W. A. Denny and L. P. G. Wakelin, *Biochim. Biophys. Acta*, 1990, **1048**, 50–58.

28 E. Tuite and B. Nordén, *J. Am. Chem. Soc.*, 1994, **116**, 7548–7556.

29 J. Sambrook, E. F. Fritsch, T. Maniatis, in *Molecular Cloning A Laboratory Manual*, Cold Spring Harbor Press, New York, 2nd edn, 1989.

30 (*a*) X. Yang and K. B. Grant, *J. Biochem. Biophys. Methods*, 2002, **50**, 123–128; (*b*) M.-J. Fernández, B. Wilson, M. Palacios, M. M. Rodrigo, K. B. Grant and A. Lorente, *Bioconjugate Chem.*, 2007, **18**, 121–129.

31 G. Cohen and H. Eisenberg, *Biopolymers*, 1969, **8**, 45–55.

32 (*a*) S. Jockusch, D. Lee, N. J. Turro and E. F. Leonard, *Proc. Natl. Acad. Sci. U. S. A.*, 1996, **93**, 7446–7451; (*b*) T. Mohammad and H. Morrison, *Bioorg. Med. Chem. Lett.*, 1999, **9**, 2249–2254; (*c*) B. Wilson, M.-J. Fernández, A. Lorente and K. B. Grant, *Tetrahedron*, 2008, **64**, 3429–3436.